JHS(E)

Full length article

The Journal of Hand Surgery
(European Volume)
2014, Vol. 39E(4) 353–363

DOI: 10.1177/1753193413505407
jhs.sagepub.com
SAGE

Unifying model of carpal mechanics based on computationally derived isometric constraints and rules-based motion – the stable central column theory

M. J. Sandow[1], T. J. Fisher[1], C. Q. Howard[2] and S. Papas[3]

Abstract

This study was part of a larger project to develop a (kinetic) theory of carpal motion based on computationally derived isometric constraints. Three-dimensional models were created from computed tomography scans of the wrists of ten normal subjects and carpal spatial relationships at physiological motion extremes were assessed. Specific points on the surface of the various carpal bones and the radius that remained isometric through range of movement were identified. Analysis of the isometric constraints and intercarpal motion suggests that the carpus functions as a stable central column (lunate–capitate–hamate–trapezoid–trapezium) with a supporting lateral column (scaphoid), which behaves as a 'two gear four bar linkage'. The triquetrum functions as an ulnar translation restraint, as well as controlling lunate flexion. The 'trapezoid'-shaped trapezoid places the trapezium anterior to the transverse plane of the radius and ulna, and thus rotates the principal axis of the central column to correspond to that used in the 'dart thrower's motion'. This study presents a forward kinematic analysis of the carpus that provides the basis for the development of a unifying kinetic theory of wrist motion based on isometric constraints and rules-based motion.

Keywords

Carpal, central column, isometric, kinematic, kinetic, motion, theory, wrist

Date received: 6th September 2012; revised: 21st August 2013; accepted: 22nd August 2013

Introduction

In an attempt to explain carpal mechanics, there have been multiple studies based on detailed empirical observation. These include *ex-vivo* cadaver studies (Short et al., 2007; Werner et al., 2005) and motion capture techniques from *in vivo* wrist data derived from computed tomography (CT) and magnetic resonance imaging (MRI) scanning (Crisco et al., 2005; Moojen et al., 2002; Moojen et al., 2003). However, these purely kinematic descriptions (Gardner et al., 2006) may not constitute usable and useful theories of carpal motion. A good theory must satisfy two requirements: '*It must accurately describe a large class of observations on the basis of a model which contains only a few arbitrary elements, and it must make definite predictions about the results of future observations*' (Hawking, 1996).

Because of the variation in carpal bone motion between wrists, a consistent and simple motion pattern has not yet been identified. It is therefore not possible to predict changes in normal and abnormal motion if such motion has not previously been studied or observed, which is in contrast to a good theory (Hawking, 1996).

Current carpal motion theories fail to achieve a consensus among researchers, are largely observational and thus poorly predictive, and are generally

[1]Department of Orthopaedics and Trauma, University of Adelaide, Adelaide, Australia
[2]Department of Engineering, University of Adelaide, Adelaide, Australia
[3]International Visualisation Centre, Adelaide, Australia

Corresponding author:
M. Sandow FRACS, Department of Orthopaedics and Trauma, Royal Adelaide Hospital, Adelaide, South Australia 5000, Australia.
Email: msandow@woc.com.au

unable to test the effect of a particular intervention in one part of the carpus on overall wrist biomechanics. Consistent with this is the observation by Moojen et al. (2003) that '*... a single functional model of carpal kinematics could not be determined*' as well as work by Galley et al., (2007) and others (Craigen and Stanley, 1995; Garcia-Elias et al., 1995; Moojen et al., 2002) who showed that there is a '*spectrum of normal carpal kinematic motion*'.

Kinematics describes the motion of bodies (objects) and systems (groups of objects) without consideration of the forces that cause the motion (Beggs, 1983; Bottema and Roth, 1979). Carpal kinematics can be seen to comprise two components.

1. Analysis (inverse) kinematics, which aims to identify the parameters and characteristics of the wrist motion to create a record of the mechanics of the wrist (Tolani et al., 2000).
2. Synthesis (forward) kinematics, which creates a model to allow predictions of spatial motion of the system components relative to each other, but not the response of the mechanical system under a load or force (Bottema and Roth, 1979; Tolani et al., 2000).

Kinetics is concerned with what causes a body to move the way it does. It relates to the effect of forces and torques on the motion of bodies having mass (Bottema and Roth, 1979; Garcia-Elias, 1997).

Previous studies have been largely observational (inverse) kinematic analyses. In contrast, rules-based motion (RBM) kinetic modelling states that the resulting motion of a solid body articulation is the net result of an applied load acting on the components of the motion system that have a defined mass, surface interaction and connections (Papas and Sandow, 2001). This mechanical concept implies the presence of four 'rules' viz: (1) bone morphology; (2) inter-bone constraints; (3) inter-bone surface interaction; and (4) applied load (Papas and Sandow, 2001).

A kinetic (rules-based) analysis identifies specific controls and constraints between the motion segments that are unique to each individual wrist. Thus, if these 'rules' can be applied to an individual wrist, where these rules have been defined, there is a greater chance that some hitherto 'unvisited' motion sequence can be predicted.

This study is as part of a bigger project to develop a unifying kinetic model of carpal motion based on computational analysis of the three-dimensional (3D) isometric constraints within the wrist, as both kinematic analysis and synthesis are required stepping stones on the way to creating the kinetic model (Bottema and Roth, 1979; Tolani et al., 2000).

While this approach may challenge some of the existing concepts, by examining the causes and controls of the carpal bones during motion, it is anticipated that a more unified theory of carpal mechanics could be developed. In reality this is likely to embrace and bring together many of the other wrist motion 'theories'.

Further, once the 'rules' are identified, the kinetic model can determine the behaviour of the system when a force is applied to the constrained objects. This model would potentially explain variances that occur in normal and injured wrists, as well as test the effect of certain reconstructive interventions.

The specific aim of this part of the project was therefore to develop a forward kinematic analysis of the carpus, which provides the basis for the development of a unifying kinetic theory of wrist motion based on isometric constraints and RBM.

Methods

The project comprised a number of discrete stages.

1. Creation of 3D models of normal wrists taken from CT scans at extremes of radial and ulnar deviation using computer surface rendering software.
2. Identification of the spatial relationships between the bones of the wrist, and in particular the identification of computer-derived isometric points between specific surfaces on individual carpal bones and between specific carpal bones and the radius.
3. Identification of the patterns of isometric relationships on the volar and dorsal aspects of the carpus.
4. Based on isometric relationships and motion patterns, development of a forward kinematic model of the wrist that could be used to help create a unifying kinetic theory of carpal motion.

Creation of 3D models

Following institutional review board authorization, CT scans (GE light speed RT8 helical scanner, GE Healthcare, UK) were performed of the right wrists of ten normal adults (eight men and two women). Their wrists were placed manually in each of the three positions at 30° of ulnar deviation, neutral and at 30° of radial deviation and saved to compact discs in a DICOM compliant format (Kabachinski, 2005). The wrist position during the CT image capture was established using a manual goniometer aligned with the long axis of the radius and the middle finger metacarpal.

The CT scans were taken at the lowest possible radiation dose (25 mAs at 120 kV) consistent with adequate image resolution and clarity. To achieve adequate image generation, approximately 105 slices (0.625 mm thick) were created for each wrist position. 3D models were generated using True Life Anatomy software (True Life Anatomy Pty Ltd, Adelaide, Australia), which creates mesh models that could be animated and manipulated within a graphics environment in an OpenGL platform. The various bones of the carpus were then separated (segmented) into the radius, ulna, scaphoid, lunate, triquetrum and trapezium. The hamate, capitate and trapezoid were not routinely individually segmented, as these bones typically function as a rigid distal row (Taleisnik, 1976).

Identification of the isometric connections between individual carpal bones and between carpal bones and the radius

The spatial relationship between various bones of the carpus and the radius were analysed. We assessed the relationships between several pairs of bones looking for isometric points between the relevant bones throughout the ranges of movement. The bone pairs were: radius and lunate; radius and triquetrum; scaphoid and lunate; lunate and triquetrum; and scaphoid and trapezium.

To emulate carpal movement and allow assessments of distance between pairs of bones in various positions of wrist motion, the bones were tracked and animated using 3D software from True Life Anatomy (True Life Anatomy Pty Ltd, Adelaide, Australia) and 3dsMax (Autodesk, Inc., California, USA).

To identify the location of isometric connections, both the dorsal and volar aspects of the respective bones were analysed using a standardized template pattern of points and numbering system. To reduce computational work, the selection of points for study was based on the likely approximate ligament attachment as described in previous cadaveric work (Berger, 2001), but without being localized to exact attachment descriptions. Between four and six points were selected on each of the bone regions, depending on the actual target area of the bone.

To validate the concept of specific locations of isometric constraints, the same template pattern of measurement points was applied to the opposite side of the bones and tested for isometricity. The extent of isometricity on the dorsal or volar aspect of certain bone pairs was then subjected to statistical analysis to establish a likelihood of isometricity occurring in a specific region on specific pairs of bones.

The distances between the selected measurement points on each of the respective paired bone surfaces was measured using the 'distance measure' and 'compare' tools in the TLA software of the three wrist positions – at 30° of ulnar deviation, in neutral and at 30° of radial deviation (Figure 1). All the measurements obtained were straight line distances, and not the distance around curved surfaces. While this may create potential measurement errors, almost all distances measured in this study were 'line of sight'. This contrasts with an assessment of the paired points that may correspond to the radio–scapho–capitate ligament, which was not part of this study. There was a complete set of all measurements for all ten wrists.

A percentage change between the maximum and minimum lengths of each such connecting line was recorded. The measurements and percentage change in length was repeated three times and for each pair of points and an average recorded. Percentage differences of < 5% were designated as isometric connections points. The isometric connections that joined isometric points on various pairs of bones were regarded as representing the net effect of ligaments that constrain motion between those bones. This generally corresponds to a specific anatomical structure, but may actually be the net result of a number of ligaments. It is important to appreciate that the actual location and position of the isometric constraints were identified not on the basis of previously described anatomical patterns but by the computer software.

Data was analysed with log binomial generalized estimating equations regression models (Liang and Zeger 1986). This was to determine whether the difference in the frequency of isometric lines between the ventral and dorsal bone regions was statistically significant. For the purpose of this analysis, isometric points were defined as those connecting lines that varied by 10% or less. The generalized estimating equations regression models were chosen, as the primary outcome is a binary variable. The analysis of these findings was based on the percentage change in length of the connection lines between the paired bone surfaces in each region, and identified that respective bony regions remained either isometric or non-isometric through the studied range of motion.

Identification of the patterns of isometric relationships of bones of the carpus

Using the 3D animation software True Life Anatomy (TLA Animator, True Life Anatomy, Adelaide, Australia) and 3ds Max (Autodesk, Inc., California, USA), the

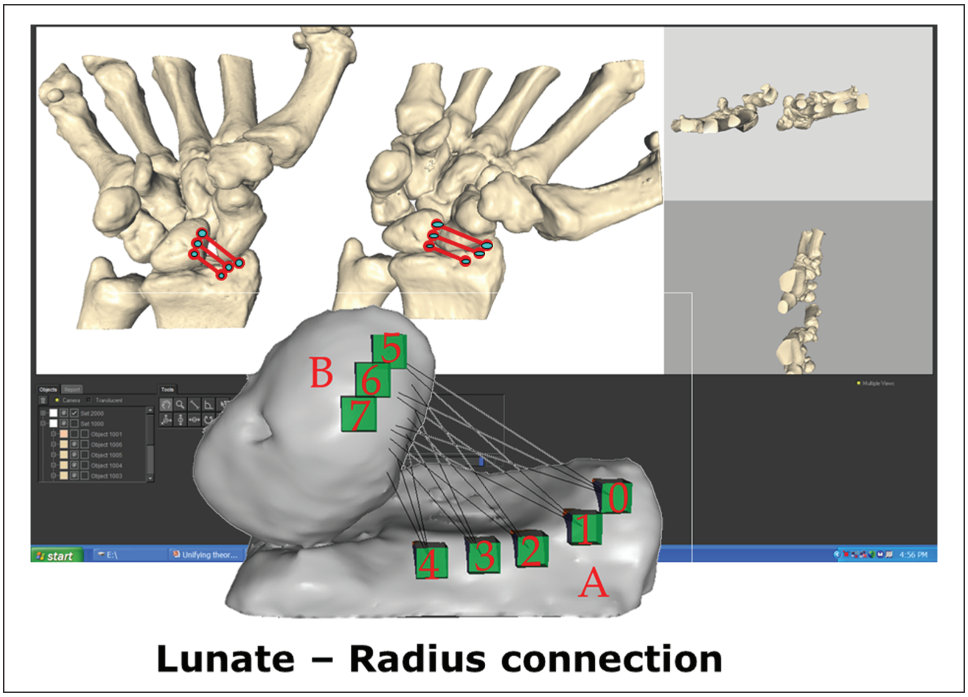

Figure 1. Example screen image generated by True Life Anatomy (True Life Anatomy Pty Ltd, Adelaide, Australia, www.truelifeanatomy.com.au) of a 3D wrist model, with the carpal bone segmented and measurement lines drawn between points on adjacent carpal bones in extremes of wrist motion. This example is of the assessment of isometricity on the volar aspect of the radius and lunate.

patterns of isometricity of each pair of bone regions studied were determined by:

(a) isometric connections only on the volar aspect;
(b) isometric connections only on the dorsal aspect;
(c) isometric connections on both the volar and dorsal surfaces of the bones.

An isometric connection on both sides implied the bones move together throughout the range of motion of the wrists for these experiments.

Based on isometric constraints and motion patterns, development of a (forward) kinematic predictive model of carpal motion

To assess the respective spatial motion of the various components of the wrist, the geometric centre of mass (centroid) of the bones (or groups of bones that moved together) of the wrist were identified by using the volumetric analysis algorithms in 3ds Max (Autodesk, Inc., California, USA), and TLA Animator (TLA Animator, True Life Anatomy, Adelaide, Australia) programs (Belsole et al., 1988). The centroid (the geometric centre of mass) is not the same as the centre of rotation, which is a point around which the object moves. For a body that moves with linear and angular motion, it is often not possible to have an instantaneous axis or point of rotation. This means that no single point in space, either within or outside the carpal bone, remains stationary through the testing range. Therefore, the most convenient method of kinematic analysis of rigid bodies in 3D space is by using the principles of relative motion of the centroids (Belsole et al., 1988). By using modelling software, 3ds Max and Adams (MSC Software Corporation, California, USA), the dynamic relationships between components of the segmented carpus were reviewed to identify movement patterns. This looked specifically at the relative motion of the centroids of the individual segments of the carpus that appeared to move differently from other segments.

Results

Isometric connections between individual carpal bones and specific carpal bones and the radius

We identified patterns of isometric constraints between carpal bones corresponding to previously described ligaments. The occurrence of isometric

Study Subject	volar Radius Lunate	dorsal Radius Lunate	volar Scaphoid Lunate	dorsal Scaphoid Lunate	dorsal Radius Triquetrum	dorsal Lunate Triquetrum	volar Lunate Triquetrum	volar Scaphoid Trapezium
1	1.48	10.44	7.95	1.80		6.50	0.97	2.09
2	4.38	5.83	14.45	1.82		6.96	9.71	2.81
3	0.15	18.66	8.28	4.01		4.72	5.12	1.15
4	2.93	6.08	9.23	5.54	5.52	13.79	6.61	4.92
5	1.22	10.04	6.88	1.45		3.63	3.09	2.32
6	3.92	3.55	1.48	5.45		8.24	3.53	5.17
7	2.10	8.27	2.82	0.57		11.71	1.21	0.03
8	1.39	14.70	1.83	2.99	11.10	14.29	1.07	4.61
9	0.87	11.25	9.94	1.25		28.36	5.36	2.84
10	2.26	7.64	5.75	0.15	8.49	6.73	3.01	2.61

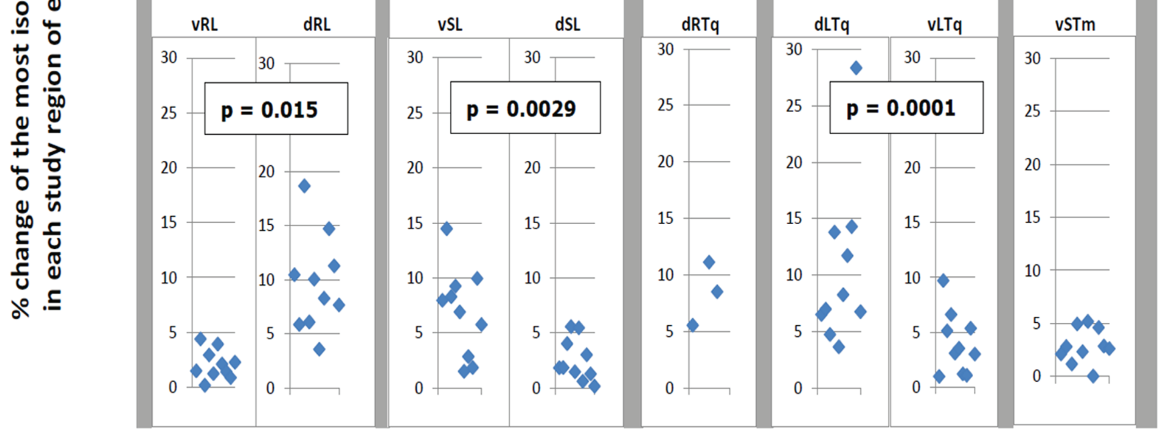

Figure 2. Average percentage change of the most isometric line joining points on the surfaces of respective bone pairs during extremes of wrist motion (at 30° of ulnar deviation, in the neutral position, and at 30° of radial deviation) in each region, in each of the 10 wrists studied. The statistical likelihood of a pair of bone surface regions being isometric is expressed as a *p* value, where volar and dorsal regions could be compared. The statistical comparison related to the frequency of a pair of regions being isometric, not the occurrence of the most isometric line between each region.

lines was concentrated in specific areas and other areas demonstrated little or no isometricity (Figure 2). There was a clear difference ($p<0.05$) between those areas (typically either volar or dorsal depending on the bones) that remained isometric and those that did not (Figure 2). The isometric points corresponded to previously documented ligament attachments (Berger, 2001).

Isometric connections were identified on the volar side of the wrist between the following joints:

- trapezioscaphoid;
- radiolunate;
- triquetrolunate.

Isometric connections were identified on the dorsal aspect of the wrist between the following joints:

- scapholunate;
- radio-triquetral.

It was not possible to measure the dorsal aspect of the trapezium and scaphoid because of overlap of the bones. In all subjects, the overall shape of the distal row (trapezoid, capitate and hamate) did not change in the various carpal positions, indicating that they move together, and can therefore be regarded as having isometricity both volarly and dorsally. Similarly, there was isometricity between the volar and dorsal surfaces of the trapezium and trapezoid, indicating that the trapezium moves with the distal carpal bones.

There was no isometricity, either volarly or dorsally, between the triquetrum and the hamate, and there was no isometricity between the volar or dorsal surfaces of the lunate and the capitate.

The relative motion and spatial relationship between the carpal bones

An analysis of the spatial relationships between the carpal bones identified a number of distinct motion

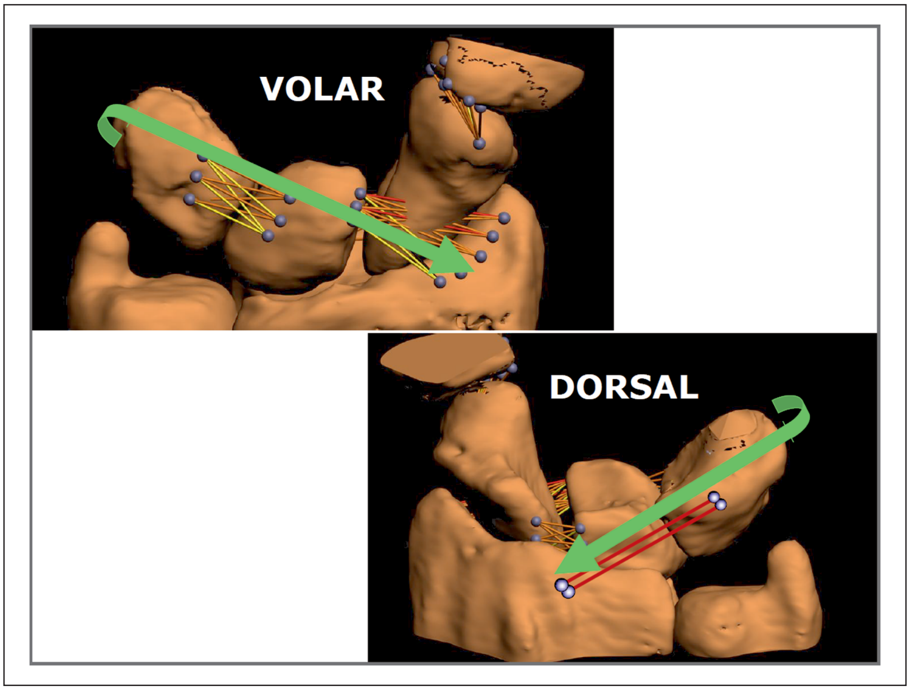

Figure 3. The triquetrum acts as an ulnar translation restraint of the proximal row of the carpus. The connection to the radius is directly via the radio–triquetral connection, and on the volar side via the interosseous ligaments attached to the lunate. The other areas of the carpus that demonstrated isometric connections are shown.

segments. Consistent with previous work by Taleisnik (1976), the capitate, hamate, trapezoid and trapezium moved as a single entity. These bones moved out of sequence with the other carpal bones (i.e. scaphoid, lunate, triquetrum and radius), which also moved relative to each other. The scaphoid, while attached to the trapezium and lunate, also moved out of sequence with other parts of the carpus, as did the triquetrum, despite its isometric attachments to the radius and lunate.

The triquetrum is connected to the radius, dorsally by the radio-carpal ligament and volarly via the lunate through the triquetrolunate and radiolunate ligaments. This would appear to give the triquetrum a role as preventing ulna translation of the carpus as it is constrained in an oblique direction to the radius both dorsally and volarly (Figure 3).

On the basis of the identified motion segments and previous work by others (Moritomo et al. 2006; Taleisnik 1976), the proximal row therefore comprised the lunate alone and the distal row comprised the capitate, hamate, trapezoid and trapezium.

It was therefore considered that the wrist could be analysed as corresponding to four distinct motion segments.

1. The distal segment (capitate – hamate – trapezoid – trapezium).
2. Lateral column (scaphoid).
3. Proximal segment (lunate).
4. Medial segment (triquetrum).

Centroids were identified in each of the motion segments. The proximal row centroid (located in the lunate) translated radially with ulnar deviation and ulnarly with radial deviation. The centroid of the distal row of carpal bones (located in the central portion of the trapezoid) moved in a radial direction with radial deviation, and ulnarly with ulnar deviation (Figure 4). Therefore the centroid of the distal and proximal rows moved in opposite directions during radial and ulnar deviation.

The translation plus rotation that occurred between the proximal and distal rows is constrained by the documented isometric connections. There are two linkages between the proximal and distal rows, one being the scaphoid's connection to the lunate and trapezium and the other through the capitolunate articulation, the latter acting as a ball and socket joint. These actual connections or articulations, plus their virtual linkages to the centroids, create four distinct arms (or bars) that form the carpus. This is more consistency with a two-geared four-bar linkage (Figure 4) rather than a slider crank mechanism. Five- and four-bar linkages are a well recognized mechanical system and can incorporate an articulating joint or meshing gear as one or more of the linkages, thus

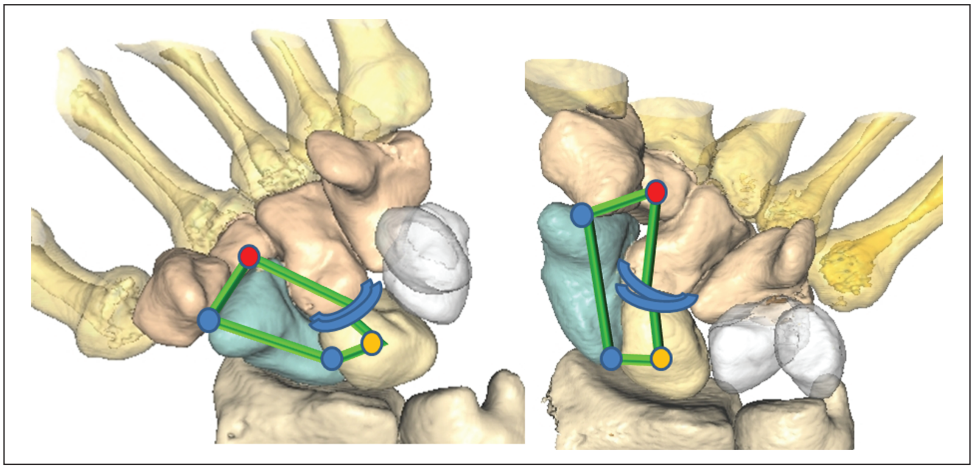

Figure 4. AP Frontal view: diagrammatic representation of the motion pattern of the carpus with overlaid linkages (as green lines) of the proximal and distal carpal row. The blue dots represent the connection points of the scaphoid to the proximal and distal rows, the red dot is the centroid of the distal row and the yellow dot is the centroid of the proximal row. The curved blue lines represent the cam motion between the two rows. The carpus appears to function as a two-gear four-bar linkage.

creating an additional linkage that provides greater power transmission with more design flexibility (Muller, 1996, Zhenying, 2011).

Motion modelling software was used to identify that the principle axis of rotation of the distal carpal row was in a plane approximately 45° pronated from the coronal plane of the radius and ulna, placing the trapezium anterior to the transverse plane of the radio-carpal joint. This appears to be in large part owing to the *trapezoid shaped* trapezoid, which rotates the principal axis of the distal row of the central column to correspond to the 'dart thrower motion' (Brigstocke et al. 2014, Crisco et al., 2005, Garcia-Elias et al. 2014, Wolfe et al., 2006).

On the basis of the apparent isometric constraints, motion patterns and axes of rotation, the carpus appears to consist of a stable central column that could provide a platform for the relatively immobile (with respect to the distal carpal row) index and middle finger metacarpals. The thenar and hypothenar rays are mobile and could act against the central metacarpals. Owing to its connections to the trapezium and lunate, the scaphoid acts as a stabilizer of the proximal and distal rows, and the triquetrum acts as an ulnar translation restraint of the proximal row, and as a controller and restraint of lunate flexion (Figures 3 and 6).

Discussion

The analysis methods used in this study have been shown to be a powerful tool for quantitative kinematic *in vivo* analysis of carpal motion, and serve to provide insights into the complexity of wrist mechanics. By a combination of oblique isometric (ligamentous) constraints, obligate translation and rotation of the carpal bones, the carpus can achieve sufficient spatial excursion with essentially two functional degrees of freedom. These ligamentous structures resist indirect rotation force delivered by the forearm muscles, creating a wrist that is stable in rotation but allows motion in other directions. Only pitch (flexion–extension) and yaw (radial and ulnar deviation) are under active control by muscular loading delivered direct to the carpus. Although some rotation through the actual carpus has been suggested, giving the wrist an extra degree of freedom as rotation (Garcia-Elias, 2008; Palmer et al., 1985), the forearm muscles are not aligned optimally to control this motion vector.

The function of the wrist can therefore be seen to allow adequate excursion in space of the relatively immobile central metacarpals (second and third) with two degrees of freedom. These metacarpals provide a post on to which the more mobile lateral (first metacarpal) and medial (fourth and fifth metacarpals) rays can work – allowing thenar and hypo-thenar opposition. The connecting lines joining these isometric points largely corresponded to the previously described interosseous and extra-osseous carpal ligaments (Berger, 1997; Berger, 2001). However, it is important to appreciate that these connecting lines were computationally derived from the serially positioned 3D carpal geometric primitives and not by using existing anatomical descriptions or knowledge.

The lunate exhibits rotational and translational excursion during wrist motion yet has no tendon

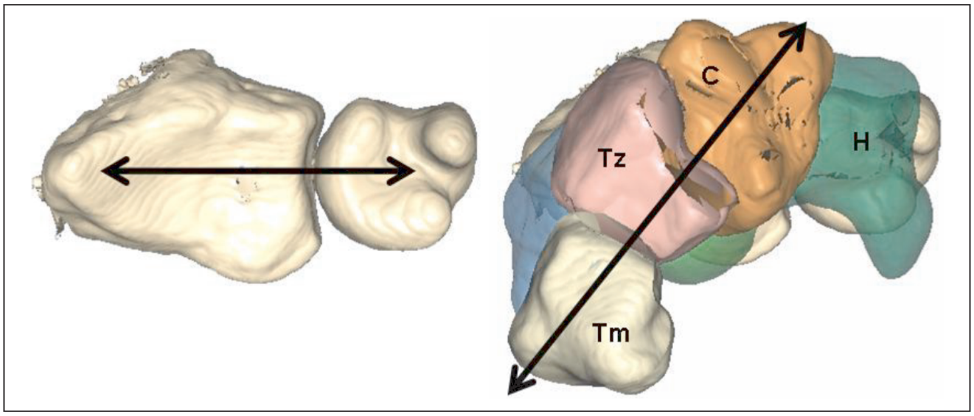

Figure 5. Axis of motion of the mid-carpal joint from the distal aspect corresponds to an angle of 45° to the transverse axis of the radius. Note the wider non-articular portion of the dorsal aspect of the trapezoid. This tends to push the trapezium anteriorly, thus rotating the prime mid-carpal motion axis in line with the dart thrower's motion.
Tm, trapezium; Tz, trapezoid; C, capitate; H, hamate.

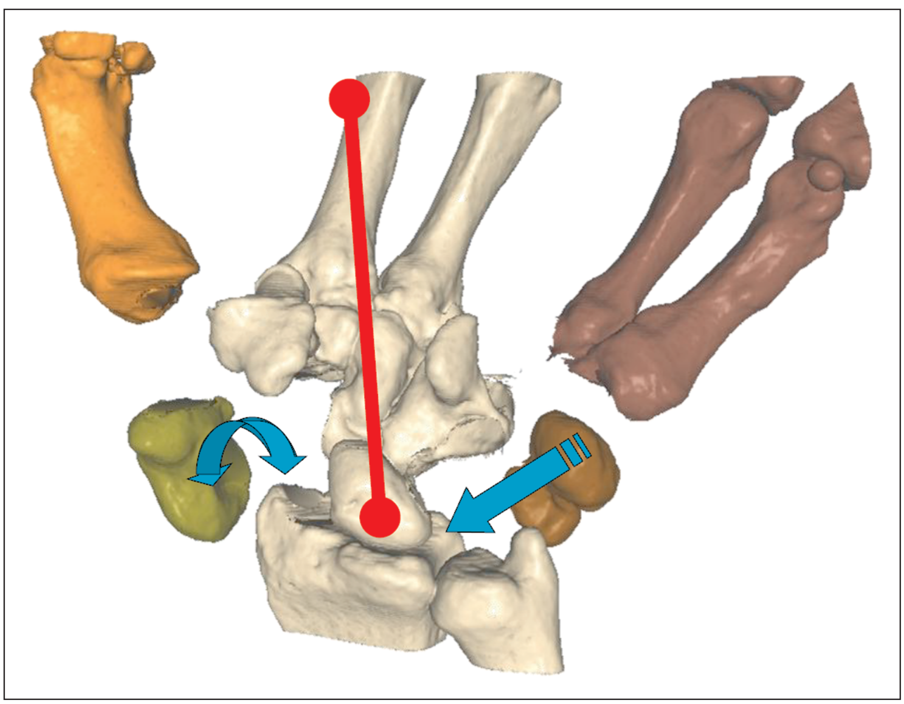

Figure 6. Stable central column theory of carpal kinetics. This consists of a stable central column that provides a platform for the relatively immobile second and third metacarpals. The thenar and hypothenar rays are mobile and act against the central metacarpals. The scaphoid acts as a stabilizer of the proximal and distal rows, and the triquetrum acts primarily as an ulnar translation restraint and as a controller and restraint of lunate flexion.

attachments. Lunate stability and motion is achieved through the obliquely orientated volar isometric constraint to the radius (corresponding to the long radiolunate ligament), which limits extension, and on the volar aspect to the triquetrum, which acts as a flexion restraint. The lunate is attached on its dorsal aspect to the scaphoid, which causes it to largely, but not completely, follow the motion of that bone. The obliquity of the various constraints (in particular the long radiolunate ligament) allows stable lunate motion through a synchronous combination of rotation and obligate translation during radial and ulnar deviation.

The 'ring theory' of Lichtman et al. (1981) suggests that the triquetrum plays an important role in stabilizing the carpus on its medial side. However, this would imply some specific connection or fixed relationship with the hamate. Our study failed to identify any isometricity between the triquetrum and hamate, and this is consistent with the recent work of Moritomo et al. (2004, 2006), suggesting the motion between these two bones does not have a fixed link, but moves in an ovoid pattern.

There was however, a very clear isometric connection between the triquetrum and the radius on the dorsal aspect, corresponding to the dorsal radio-carpal ligament (Viegas, 2001), and indirectly via the lunate on the volar aspect. This suggests the triquetral connections are ideally suited to act as an ulnar translation restraint of the proximal row of the carpus, rather than having any direct role in vertical carpal stability (Figure 3). The connection to the triquetrum on the volar aspect to the lunate is also ideally suited to control lunate flexion. Triquetral flexion is in turn controlled by the dorsal radio-carpal ligament. The triquetrum thus contributes to vertical carpal stability, but only by its connection to the volar aspect of the lunate, and not with any specific linkage to the medial carpus or, more specifically, the hamate.

Our findings contrast with the work by Xu and Tang (2009), who were unable to identify isometric connections between the carpal bones. The difference may be the inaccuracy owing to their manual selection of measurement points based on anatomical descriptions of ligament attachment. As distinct from Xu and Tang (2009), clear evidence of isometricity (<5% variation) was identified, and this generally corresponded to the described ligament structures. It was evident that even minor variation in the position of the selected points on the surfaces of the bones to be assessed created quite large variation in connecting line length in the different wrist positions. As such, the existing description of ligamentous attachment may not exactly reflect the isometric points between various bones of the carpus in different individuals.

It should be noted however, that the simplicity of straight isometric lines measured between bone surfaces may not entirely represent the actual interactions occurring within the carpus. Many ligaments do not run in straight lines, as they may at times pass over convex bone surfaces. Such interactions involving multiple other ligaments and the carpal bones should be considered in future work. The regions assessed in this study were largely connected by lines that did not have an intervening convex bony surface, and further, measuring around curves was outside the scope and software capabilities of this study.

On the basis of the computationally derived isometric constraints and inter-row motion identified in this study, the carpus appears to function as a stable central column (lunate–capitate–hamate–trapezoid–trapezium) with a supporting lateral column (scaphoid). The carpus can be seen as a closed linkage joining the radius to the bases of the metacarpals, achieving the required motion and stability. The carpus itself functions much more like a 'two–gear four-bar linkage' (Figure 4) than the traditionally described 'slider crank'. On the medial side of the central column, the triquetrum acts principally as an ulnar translation restraint, counteracting the tendency of the carpus to slide down the obliquity of the distal radius (Figure 6). This is very similar to Taleisnik (1976) and earlier Navarro (1921), but with a more defined supporting lateral column (scaphoid) creating a four-bar linkage (incorporating two gears) – upon which tendons would act to achieve motion.

The 'trapezoid'-shaped trapezoid places the trapezium anterior to the transverse plane of the radius and ulna, and thus rotates the principal axis of the central column, and more specifically the mid-carpal joint, to correspond to that used in the dart thrower motion. This arc of motion change allows for obliquity of the palm for gripping objects parallel to the forearm, thus co-linearly extending the upper limb, which has major implications with respect to tool use. A variation in the shape of the trapezoid alters the prime axis of the rotation of the distal row, and may thus explain cross-species variations in wrist function, particularly the ability to throw darts (Crisco et al., 2005; Wolfe et al., 2006). The anterior positioning of the trapezium and the attached thumb metacarpal may also facilitate tool use by allowing thumb pad to index finger pad holding, a function that is possible in humans but not in chimpanzees (Marzke, 2009; Young, 2003).

The concept of the stable central column of carpal motion provides the basis for the development of a truly kinetic motion theory using the RBM system, extending the central column concept described by Taleisnik (1976). This is consistent with the ideals of a good theory in that it provides a simplified description of a mechanical system based on isolated observations, it is predictive and it can be tested (Hawking, 1996). It unifies the mechanical observations derived from a range of previous researchers, in particular the intercalated segment motion of the lunate (Berger, 1997), the ovoid motion of the mid-carpal joint (Moritomo et al., 2004) and, more recently, the dart thrower motion concept (Crisco et al., 2005; Moritomo et al., 2007).

By identifying the derived and implied rules of a particular wrist, proposed reconstructive procedures could potentially be applied to the mathematical model to predict actual outcomes in a particular patient or injury pattern. In the future, this may be able to identify the most appropriate reconstructive or repair procedure for the individual wrist with a particular injury pattern. Further work will be needed to develop and apply the kinetic theory to a range of injuries and validate the use of this quantitative analysis technology to plan more mechanically based treatments.

Acknowledgements

We wish to thank the many researchers in wrist mechanics whose presentations and discussions, both informally and as part of the International Wrist Investigators Workshop, contributed to defining the issues and challenges of carpal mechanics, and in particular Dr Marc Garcia-Elias (Barcelona, Spain), Dr Dick Berger (Mayo Clinic, USA) and Dr Scott Wolfe (New York, USA). We also wish to thank True Life Anatomy for the technology support, and Drs Stephen Tham and De Juan Ng, for access to patient CT scan data.

Conflict of interests

M. J. Sandow and S. Papas have received or may receive a benefit from a commercial party related to the content of this study. The other authors have no conflicts of interest to declare.

Funding

This research received no specific grant from any funding agency in the public, commercial, or not-for-profit sectors.

References

Beggs JS. *Kinematics*. Washington, Hemisphere Pub. Corp, 1983: 1.

Belsole RJ, Hibelink DR, Llewellyn JA, Stenzier S, Greene TL, Dale M. Mathematical analysis of computed carpal models. J Orthop Res. 1988, 6: 116–22.

Berger RA. The ligaments of the wrist. A current overview of anatomy with considerations of their potential functions. Hand Clin. 1997, 13: 63–82.

Berger RA. The anatomy of the ligaments of the wrist and distal radioulnar joints. Clin Orthop Relat Res. 2001, 383: 32–40.

Bottema O, Roth B. *Theoretical kinematics*. New York, Dover Publications, 1979: vii, 299.

Brigstocke GHO, Hearnden A, Holt C and Whatling G. *In-vivo* confirmation of the use of the dart thrower's motion during activities of daily living. J Hand Surg Eur. 2014, 39: 373–378.

Craigen MA, Stanley JK. Wrist kinematics. Row, column or both? J Hand Surg Br. 1995, 20: 165–70.

Crisco J, Coburn JC, Moore DC, Akelman E, Weiss APC, Wolfe SW. In vivo radiocarpal kinematics and the dart thrower's motion. *J Bone Joint Surg Am*. 2005, 87: 2729–40.

Galley I, Bain GI, McLean JM. Influence of lunate type o scaphoid kinematics. J Hand Surg Am. 2007, 32: 842–7.

Garcia-Elias M. Kinetic analysis of carpal stability during grip. Hand Clinics. 1997, 13: 151–8.

Garcia-Elias M. The non-dissociative clunking wrist: a personal view. J Hand Surg Eur. 2008, 33: 698–711.

Garcia-Elias M, Ribe M, Rodriguez J, Cots M, Casas J. Influence of joint laxity on scaphoid kinematics. J Hand Surg Br. 1995, 20: 379–82.

Garcia-Elias M, Alomar Serrallach X, Monill Serra J. Dart-throwing motion in patients with scapholunate instability: a dynamic four-dimensional computed tomography study. J Hand Surg Eur. 2014, 39: 346–352.

Gardner MJ, Crisco JJ, Wolfe SW. Carpal kinematics. Hand Clin. 2006, 22: 413–20.

Hawking S. The illustrated brief history of time (Updated and expanded). New York, Bantam Books, 1996: 15.

Kabachinski J. DICOM: key concepts-part I. Biomed Instrum Technol. 2005, 39: 214–16.

Liang K-Y, Zeger SL. Longitudinal data analysis using generalized linear models. Biometrika. 1986, 73(1): 13–22.

Lichtman DM, Schneider JR, Swafford AR, Mack GR. Ulnar midcarpal instability-clinical and laboratory analysis. J Hand Surg Am. 1981, 6: 515–23.

Marzke MW. Upper-limb evolution and development. J Bone Joint Surg Am. 2009, 91: 26–30.

Moojen TM, Snel JG, Ritt MJ, Kauer JM, Venema HW, Bos KE. Three-dimensional carpal kinematics in vivo. Clin Biomech. 2002, 17: 506–14.

Moojen TM, Snel JG, Ritt MJ, Venema HW, Kauer JM, Bos KE. In vivo analysis of carpal kinematics and comparative review of the literature. J Hand Surg Am. 2003, 28: 81–7.

Moritomo H, Apergis EP, Herzberg G, Werner FW, Wolfe SW, Garcia-Elias M. 2007 IFSSH committee report of wrist biomechanics committee: biomechanics of the so-called dart-throwing motion of the wrist. J Hand Surg Am. 2007, 32: 1447–53.

Moritomo H, Murase T, Goto A, Oka K, Sugamoto K, Yoshikawa H. In vivo three-dimensional kinematics of the midcarpal joint of the wrist. J Bone Joint Surg Am. 2006, 88: 611–21.

Moritomo H, Murase T, Goto A, Oka K, Sugamoto K, Yoshikawa H. Capitate-based kinematics of the midcarpal joint during wrist radioulnar deviation: an in vivo three-dimensional motion analysis. J Hand Surg Am. 2004, 29: 668–75.

Muller M. A novel classification of planar four-bar linkages and its application to the mechanical analysis of animal systems. Phil Trans R Soc Lond B. 1996, 351: 689–720.

Navarro A. Luxaciones del carpo. Anal Fac Med. 1921, 6: 113–41.

Palmer AK, Werner FW, Murphy D, Glisson R. Functional wrist motion: a biomechanical study. J Hand Surg Am. 1985, 10: 39–46.

Papas S and Sandow MJ. (True Life Creations (S.A.) Pty Ltd, Australia): Animation technology. US Patent 7,236,817, 5 March 2001.
Short WH, Werner FW, Green JK, Sutton LG, Brutus JP. Biomechanical evaluation of the ligamentous stabilizers of the scaphoid and lunate: part III. J Hand Surg Am. 2007, 32: 297–309.
Taleisnik J. The ligaments of the wrist. J Hand Surg Am. 1976, 1: 110–18.
Tolani D, Goswami A, Badler NI. Real-time inverse kinematic techniques for arthropomorphic limbs. Graphical Models. 2000, 62: 353–88.
Viegas SF. The dorsal ligaments of the wrist. Hand Clin. 2001, 17: 65–75.
Werner FW, Short WH, Green JK. Changes in patterns of scaphoid and lunate motion during functional arcs of wrist motion induced by ligament division. J Hand Surg Am. 2005, 30: 1156–60.
Wolfe SW, Crisco JJ, Orr CM, Marzke MW. The dart-throwing motion of the wrist: is it unique to humans? J Hand Surg Am. 2006, 31: 1429–37.
Xu J, Tang JB. In vivo length changes of selected carpal ligaments during wrist radioulnar deviation. J Hand Surg Am. 2009, 34: 401–8.
Young RW. Evolution of the human hand: the role of throwing and clubbing. J Anat. 2003, 202: 165–74.
Zhenying Y. *Composite mechanisms*. Victoria, Canada, Trafford Publishing, 2011: 2.